

In situ Ultrasound-Assisted Etching of <100> Si Wafers by KOH

Vassili Karanassios*, Jonathan T. Sharples and Arokia Nathan¹

Guelph-Waterloo Center for Graduate Work in Chemistry, Department of Chemistry,
University of Waterloo, Waterloo, Ontario, Canada N2L 3G1

¹Department of Electrical and Computer Engineering, University of Waterloo
Waterloo, Ontario, Canada N2L 3G1

(Received June 3, 1996; accepted September 16, 1996)

Key words: ultrasound, etching, surface smoothness, sonochemistry, chemical microinstrumentation

Surface quality and the amount of residue remaining on a <100> Si wafer after anisotropic, wet chemical etching is of concern when micromachining relatively deep (*e.g.*, > 20 μm), flat-bottomed or V-shaped microchannels. In this work, ultrasound-assisted anisotropic etching using a 20% solution of KOH at 65°C was employed for the development of such microchannels, and the results were compared with those obtained using magnetic stirring. It was found that ultrasound-assisted etching improves the quality of the etched surfaces, reduces the amount of residue remaining on the wafer after etching and results in faster etch rates. These improvements were attributed to an increase in mass transfer during etching and to an enhancement of reactivity as a consequence of sonochemistry.

1. Introduction

Over the last two decades, there has been an increasing amount of interest in the use of crystalline-Si (c-Si) as a mechanical material⁽¹⁾ for the development of microstructures ranging from sensors, actuators^(1–5) and micro electro mechanical systems (MEMS)^(6,7) to chemical microinstruments.^(7–10) For chemical microinstruments in particular and, similar to their large-scale counterparts, there are many instances in which a liquid or a gaseous sample must be transported from one part of a microstructure to another, for example, from

* Author to whom correspondence should be addressed.

an inlet to a sensing element to an outlet. However, unlike the large-scale counterparts, transport of samples usually takes place using relatively deep (*e.g.*, $>20\ \mu\text{m}$), flat-bottomed microchannels (Fig. 1) which are etched on c-Si, typically using anisotropic wet chemical etchants.

Although Si micromachining of $\langle 100 \rangle$ wafers using an anisotropic etchant, such as KOH,^(1,2,11-17) is an effective means of producing microchannels (Fig. 1), it also produces some undesirable side effects. For example, it results in rough bottom surfaces^(2,13,18) and, especially at relatively low temperatures (*e.g.*, $<70^\circ\text{C}$), it leaves a residue on the wafer (Fig. 2a). These drawbacks have been attributed to an inability to remove the reaction products rapidly and/or completely⁽¹³⁾ and to poor dissolution of the product(s) that form the residue. In addition, pyramidal protrusions (Fig. 2b), whose facets are bound by the $\langle 111 \rangle$ ⁽¹⁹⁻²¹⁾ or by the $\langle 411 \rangle$ ⁽²¹⁾ planes, often form at the bottom of etched microchannels, most notably when relatively deep etches are employed. These 'hillocks' or pyramids are thought to form on structural defects⁽²²⁾ that depend on the thermal and stress history of the wafer or on impurities of c-Si that lead to local passivation. Alternatively, they have been considered⁽¹³⁾ a consequence of nucleation site formation due to local passivation. Local passivation, in turn, is a result of either an inability to etch microspots, or inefficient mass transfer during etching, or both. These undesirable side-effects of etching undermine the mechanical integrity of microstructures and may even adversely affect chemical composition and flow patterns of gaseous or liquid samples in a microchannel as they travel from inlet to outlet.

One way of increasing mass transfer and chemical reactivity during etching is by using ultrasound to agitate the etchant solution rather than magnetic stirring. In this work, preliminary results obtained using ultrasound-assisted wet chemical etching of n-doped (phosphorus), 3-inch $\langle 100 \rangle$ Si wafers of 1–2 $\Omega\cdot\text{cm}$ resistivity using a 20% aqueous KOH etchant solution at 65°C are described and compared with results obtained using magnetic stirring.

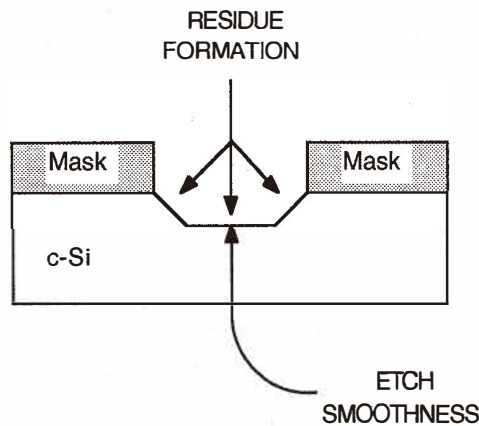


Fig. 1. Cross section of a flat-bottomed microchannel.

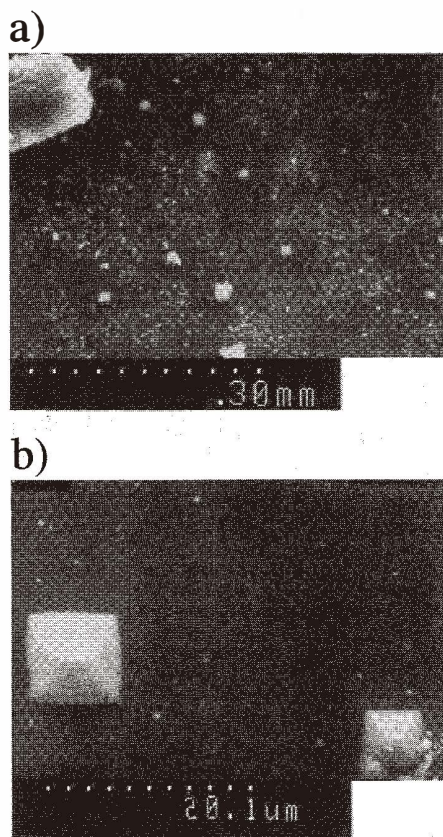


Fig. 2. Scanning electron micrographs of the bottom of a channel of a magnetically stirred etched wafer showing a) residue and pyramids and b) close up of a pyramidal structure.

2. Background

The $\langle 100 \rangle$ crystallographic orientation was chosen due to its wide applicability to MEMS as a result of its unique anisotropic etching properties.^(1,2) In anisotropic etching, the etch rate varies with the crystallographic orientation and, for KOH, the etch rate of the $\langle 100 \rangle$ planes may be as high as 400 times that of the $\langle 111 \rangle$ planes.⁽¹⁷⁾ The resultant structure depends, among others, on geometry and orientation of the mask opening, wafer thickness, dopant species and concentration, defects/impurities of c-Si and etching conditions (*e.g.*, time, temperature, etchant concentration). For the same etch depth and for rectangular mask openings, a wide opening results in a flat-bottomed channel (Figs. 3a to 3d) whereas a narrow opening results in a V-grooved channel (Figs. 3a' to 3d'). In both cases, the side-walls are V-shaped and are defined by the slow-etching $\langle 111 \rangle$ planes.

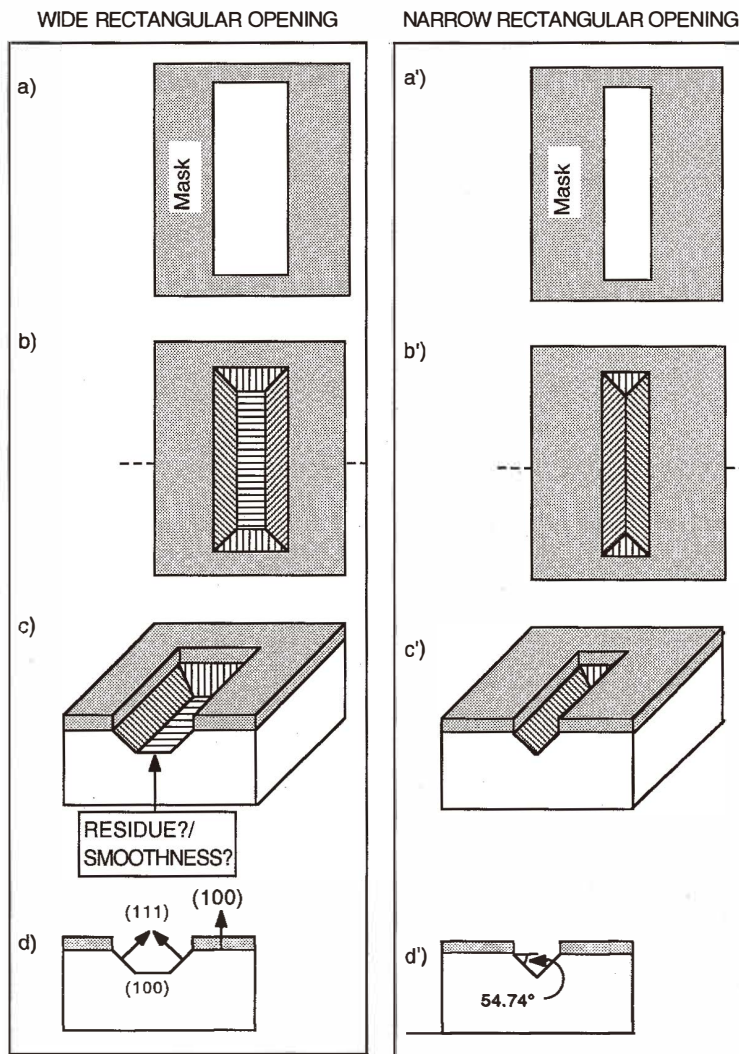


Fig. 3. Anisotropic etching behavior of (100) silicon: a) and a') mask opening, b) and b') top view after etching, c) and c') 3d views of flat-bottom and of V-grooved microchannels, and d) and d') cross sections of the channels shown in c) and c'). In general, etching will stop automatically when the (111) planes meet (as shown in d') and the flat bottom defined by the (100) plane (c and d) disappears. For simplicity, undercutting of the mask by the etchant solution is not shown.

Vertical walls can be obtained by using $\langle 110 \rangle$ wafers⁽¹⁾ or $\langle 100 \rangle$ wafers,⁽²³⁾ the latter requiring an unusual mask alignment and a high concentration of KOH.

Of the several wet anisotropic etchants, for example, solutions of CsOH, NaOH or

KOH, ethylene diamine-pyrocatechol-water (EDP), tetramethyl ammonium hydroxide (TMAH) or hydrazine (NH_2NH_2), KOH was chosen. This is a widely used etchant,⁽¹⁶⁾ despite its tendency to attack masking materials, Al metallization and a lack of fundamental understanding of its exact etching mechanism.^(1,2,11-16) A generalized reaction scheme for wet chemical etching by KOH involves attack of the exposed silicon surface followed by removal and dissolution of the products of the etching reaction. Conceptually, this occurs in three simple steps:

- i) the reactants are transported from the bulk of the solution to the exposed Si surface,
- ii) a reaction occurs at the surface,
- iii) the products of the etching reaction are transported away from the surface into the bulk of the solution.

One way of improving mass transfer and increasing reactivity is using ultrasound technology.⁽²⁴⁻³⁰⁾

Ultrasound has been defined as “any sound which is of a frequency beyond that to which the human ear can respond, i.e., above 16 kHz”.⁽²⁴⁾ Typically, it is generated by applying an alternating voltage across a piezoelectric material. Devices that emit high-frequency (e.g., 2–10 MHz), low-amplitude sound waves are used, for example, in medical imaging for diagnostic purposes. Those that emit low-frequency (e.g., 20–100 kHz), high-amplitude sound waves are referred to as power ultrasound devices.⁽²⁴⁾ Commercially available ‘power’ sonicators are widely used in chemical laboratories; for example, to mix solutions. Improved mixing and increased mass transfer of the etchant solution and enhanced removal of the products of the etching reaction were expected when using ultrasound, thus affecting steps i) and iii) above.

Increased reactivity in liquid-solid interactions has been reported⁽²⁵⁻²⁹⁾ when a liquid is irradiated with power ultrasound. Acoustic cavitation,⁽³⁰⁾ that is, “the creation, expansion and implosive collapse”⁽³¹⁾ of microbubbles ($\sim 100 \mu\text{m}$) created by ultrasonic waves, generates extreme conditions (e.g., $\sim 5,000^\circ\text{C}$ and ~ 500 atmospheres) in transient microspots⁽²⁷⁻²⁹⁾ and is considered to be the source of increased reactivity and the foundation of sonochemistry.⁽²⁴⁻²⁶⁾ As a consequence of cavitation, sonochemistry was expected to affect the second step, to enhance the etch rate and to help improve dissolution of the product(s) that form a residue.

3. Experimental

A thick oxide layer was thermally grown on a wafer that was subsequently patterned with rectangles of varying dimensions. The working area of each wafer was approximately 1.1×1.1 in. Prior to immersion in the etchant solution, each wafer was placed in a dilute aqueous solution of hydrofluoric acid (3% HF) for approximately 45 s. This was followed by a thorough rinse with a stream of distilled, deionized water. The HF rinse served to remove the thin layer of native oxide on the exposed Si surface while leaving the mask material relatively unharmed.

The HF-rinsed wafer was mounted on an in-house constructed holder that was placed in a covered etch-bath beaker in the vertical direction (Fig. 4). All etching took place in a

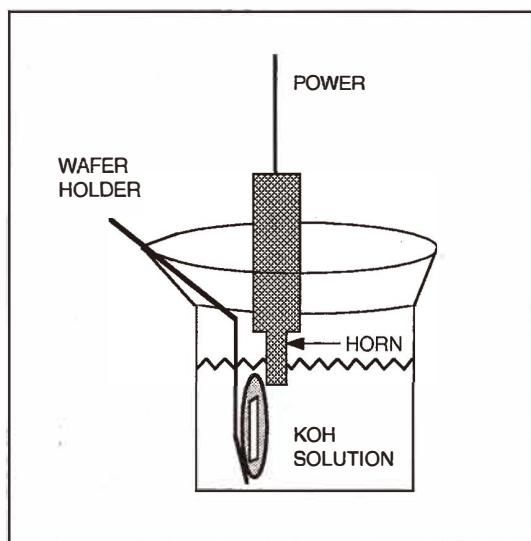


Fig. 4. Experimental set up for *in situ* ultrasound-assisted wet chemical etching. Illustration not to scale.

class 1,000 clean room and lasted for 100 min to ensure an etch depth of $> 20 \mu\text{m}$. Also, the same artificial light conditions were used throughout, since illumination is known to influence etching by creating electron-hole pairs on the etched surface(s). The temperature of the etchant solution was kept constant at 65°C . Although the relatively low temperature helps preserve the integrity of other structures or materials on the wafer, it also encourages formation of a large amount of residue.

For the ultrasound experiments, a Tekmar (model TM600) 'power' sonicator operating at a fixed frequency of 20 kHz and with a maximum power output of 600 W was used. To test the effectiveness of the approach, the tip of the ultrasonic horn was positioned approximately 1 cm below the surface of the etchant solution (Fig. 4). The top of the wafer was located approximately 1.5 cm below the tip of the horn with the long side of the rectangular mask opening positioned parallel to the horn.

Power output was 85% of full scale and the duty cycle was 60%. The etchant solution was heated to 65°C before the sonicator horn was immersed in it. Power was applied to the sonicator and, to offset heating of the etchant solution by ultrasound, the etchant solution was thermostated to $\pm 0.5^\circ\text{C}$ to maintain a constant temperature. It should be noted that the Ti sonicator horn is susceptible to erosion in alkaline solutions at temperatures above about 75°C and that delicate structures such as microbridges may necessitate the use of low power levels to avoid damage.

For the experiments in which a magnetic stirrer was used, the etchant solution was thermostated using a hot plate with feedback temperature control ($\pm 0.5^\circ\text{C}$). Also, a

chemically inert stirring bar was used and the stir rate was set to the maximum allowable setting for this hot plate (Corning, model PC-351).

The etched surfaces were examined qualitatively using optical and video microscopy and scanning electron microscopy (SEM, magnification up to 15,000 times). Quantitative etch-depth and surface-roughness results were obtained using a mechanical stylus profilometer (Dektak) whose traces were plotted using a chart recorder.

4. Results and Discussion

Ultrasound-assisted etching resulted in smoother surfaces as compared to magnetic stirring. Examples of the digitized Dektak traces of the etched surface profile are shown in Fig. 5. The standard deviation of these traces was used as a quantitative measure of surface roughness. On average and for the same etch time, surface roughness for the ultrasonically agitated wafer was $0.25\ \mu\text{m}$ at a depth of $58\ \mu\text{m}$ and $0.70\ \mu\text{m}$ at a depth of $26\ \mu\text{m}$ for the magnetically stirred wafer. Improvements in surface roughness have been reported by others for shallower etch depths by immersing the beaker containing the wafer and the etchant solution into an ultrasonic bath.^(18,32,33)

Qualitative observations further corroborate surface roughness measurements. For example, the wafer etched using a magnetically stirred etchant solution had a rough surface with pyramids (Fig. 2b) and a white residue (Fig. 2a) that was visible even to a naked eye. In contrast, pyramids were not observed and the amount of residue was clearly reduced when ultrasound was used. Although the residue may be removed by thorough rinsing, this adds additional processing steps and, depending on the amount of residue, it may necessitate the use of solvents that are not compatible with other structures on the wafer. There was also an increase in the etch rate of 2.2 times when ultrasound was used. Similar improvements were noted by etching at 65°C with a 4 M KOH solution in an ultrasonic cleaning bath.⁽¹⁸⁾

5. Conclusions

The preliminary results reported in this work show that, in contrast to magnetic stirring, *in situ* ultrasound-assisted anisotropic etching of $\langle 100 \rangle$ wafers using 20% KOH at 65°C results in smoother surfaces at the bottom of etched microchannels, reduces the amount of residue remaining on the wafer and increases the etch rate. Most likely, these improvements are a result of the increased mass transfer and enhanced reactivity induced by ultrasound. The results of this work and those reported by others for $\langle 110 \rangle$ wafers and different experimental conditions^(32,33) indicate a more general applicability of ultrasound-assisted, anisotropic wet chemical etching, thus warranting further investigation.

For instance, future work may involve a systematic study of the effect of power ultrasound on surface quality and etch rate as a function of etching variables, such as etchant composition, temperature, pH, wafer and crystallographic orientation, not only for KOH but for other etchants as well. These include EDP⁽³⁴⁾ (which is an etchant that shows

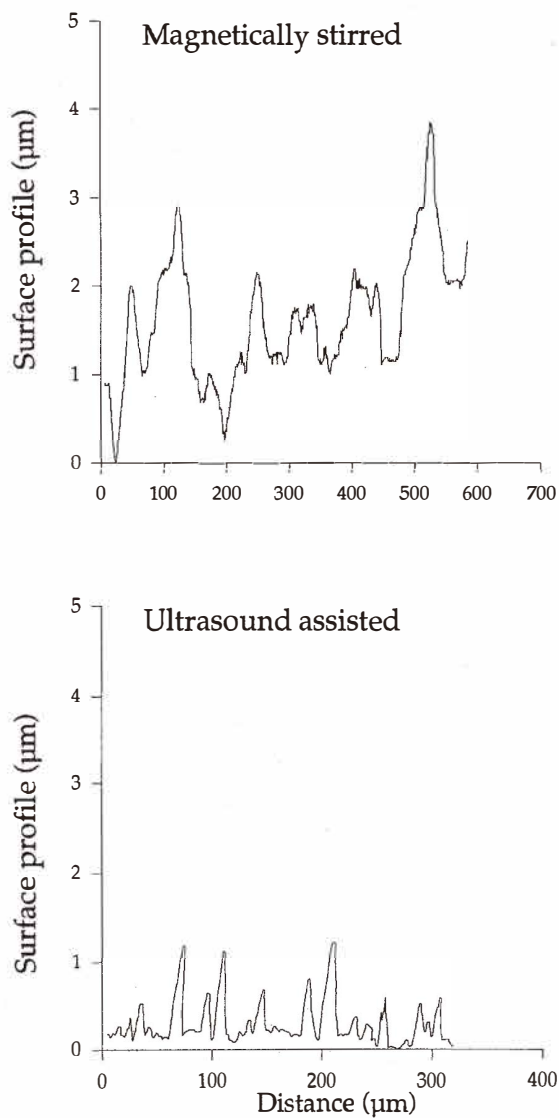


Fig. 5. Digitized Dektak traces of the surface profile of the flat bottom (Fig. 2d) of an etched microchannel (with zero defined as the deepest part of the channel) for the magnetically stirred and sonicated solutions.

greater dependence on diffusion than $\text{KOH}^{(11)}$ and ammonium-based solutions,^(35,36) which are compatible with commercial CMOS processes⁽³⁷⁾ but have a tendency to form pyramids under certain experimental conditions.⁽³⁴⁻³⁶⁾ The results of such investigations may provide

additional insights into the underlying mechanism(s) of wet anisotropic chemical etching and may extend the range of applications of micromachining. Examples include deep etches for micromolding⁽³⁸⁾ and microstructures in which c-Si is used, not only as a mechanical material (e.g., pressure sensors or microfluidic systems), but also as optical^(32,39) and electronic (e.g., integrated MEMS or iMEMS⁽⁴⁰⁾) material as well. Potentially, they may even aid the development of integrated chemical MEMS (icMEMS).

Endnote

Part of this work was reported in an undergraduate thesis (Chem 492) by JTS in partial fulfillment of a requirement for an honours B. Sc. degree in Chemistry (April 1993). Financial assistance from the University of Waterloo is also gratefully acknowledged.

References

- 1 K. E. Petersen: Proc. IEEE **70** (1982) 420.
- 2 J. C. Greenwood: J. Phys. E: Sci. Instrum. **21** (1988) 1114.
- 3 W. H. Ko and M. Mehregany: Sensors and Materials **3** (1992) 293.
- 4 A. van den Berg, P. D. van der Wal, B. H. van der Schoot and N. F. de Rooij: Sensors and Materials **6** (1994) 23.
- 5 J. Janata, M. Josowicz and D. M. DeVaney: Anal. Chem. **66** (1994) 207R.
- 6 R. S. Muller: Sensors and Actuators A **21–23** (1990) 1.
- 7 K. J. Gabriel: Sci. American **273** (September 1995) 150.
- 8 J. B. Angel, S. C. Terry and P. W. Barth: Sci. American **248** (April 1983) 44.
- 9 A. Manz, J. C. Fettinger, E. Verpoorte, H. Lüdi, H. M. Widmer and D. J. Harrison: Trends in Anal. Chem. **10** (5) (1991) 144.
- 10 G. T. A. Kovacs, K. Petersen and M. Albin: Anal. Chem. **68** (1996) 407A.
- 11 H. Seidel, L. Csepregi, A. Heuberger and H. Baumgartel: J. Electrochem. Soc. **137** (1990) 3612.
- 12 H. Seidel, L. Csepregi, A. Heuberger and H. Baumgartel: J. Electrochem. Soc. **137** (1990) 3626.
- 13 E. D. Palik, O. J. Glembocki, I. Heard, Jr., P. S. Burno and L. Tenerz: J. Appl. Phys. **70** (1991) 3291.
- 14 M. Elwenspoek: J. Electrochem. Soc. **140** (1993) 2075.
- 15 K. E. Bean: IEEE Trans. on Electron Dev. **ED25** (1978) 1185.
- 16 I. Stoev: Sensors and Actuators A **51** (1996) 113.
- 17 G. Delapierre: Sensors and Actuators A **17** (1989) 123.
- 18 A. Kuntman: J. Mat. Sci. Letters **11** (1992) 1274.
- 19 E. D. Palik, V.M. Bermudez and O. J. Glembocki: J. Electrochem. Soc. **132** (1985) 871.
- 20 H. L. Offereins, K. Kühn and H. Sandmaier: Sensors and Actuators A **25–27** (1991) 9.
- 21 H. L. Offereins, H. Sandmaier and K. Marusczyk: K. Kühn and A. Plettner **3** (1992) 127.
- 22 Y. K. Bhatnagar, A. Nathan and Y. Lu: Sensors and Materials **7** (1996) 423.
- 23 L. Tenerz, Y. Backlund, J. Tirén and J. O'Connell: Sensors and Materials **1** (1989) 313.
- 24 T. J. Mason (Ed.): Chemistry with Ultrasound (Elsevier Applied Science, NY, 1990).
- 25 T. J. Mason and J. P. Lorimer: Sonochemistry: Theory, applications and uses of ultrasound in chemistry, Ellis Horward, Chichester (1988).
- 26 K. S. Suslick (Ed.): Ultrasound: Its chemical, physical and biological effects (VCH, NY, 1988).

- 27 S. J. Doktycz and K. S. Suslick: *Science* **247** (1990) 1067.
- 28 K. S. Suslick: *Sci. American* **260** (February 1989) 80.
- 29 K. S. Suslick and E. B. Flint: *Nature* **330** (1987) 553.
- 30 R. E. Apfel: Chapter 7 in *Methods of Experimental Physics, Volume 19: Ultrasonics*, ed. P. D. Edmonds (Academic Press, NY, 1981).
- 31 K. S. Suslick, D. A. Hammerton and R. E. Cline, Jr.: *J. Am. Chem. Soc.* **108** (1986) 5641.
- 32 S. W. Smith, M. Mehregany, F. Merat and D. A. Smith: *SPIE* **2686** (1996) 17.
- 33 K. Ohwada, Y. Negoro, Y. Konaka and T. Oguchi: *Sensors and Actuators A* **50** (1995) 93.
- 34 Y. K. Bhatnagar and A. Nathan: *Sensors and Actuators A* **36** (1993) 233.
- 35 U. Scnakerenberg, W. Benacke and B. Lochel: *Sensors and Actuators A* **25–27** (1991) 1.
- 36 O. Tabata, R. Asahi, H. Funabashi, K. Shimaoka and S. Sugiyama: *Sensors and Actuators A* **34** (1992) 51.
- 37 H. Baltes: *Sensors and Actuators A* **37–38** (1993) 51.
- 38 Y. Xia, E. Kim, X. M. Zhao, J. A. Rogers and G. M. Whitesides: *Science* **273** (1996) 347.
- 39 A. Klumpp, K. Kühn, U. Schaber, H. U. Kaaulf and W. Lang: *Sensors and Actuators A* **51** (1995) 77.
- 40 H. Baltes: *Sensors and Materials*, this issue,